Title

Super-Resolution Stimulated Raman Scattering Microscopy with Graphical User Interface—Supported A-PoD

Journal

Current Protocols, 4(1)

ISSN

2691-1299

Authors

Jang, Hongje

Li, Yajuan

Wu, Shuang

et al.

Publication Date

2024

DOI

10.1002/cpz1.970

Peer reviewed

Super-Resolution Stimulated Raman Scattering Microscopy with Graphical User Interface–Supported A-PoD

Hongje Jang,[1] Yajuan Li,[1] Shuang Wu,[1] and Lingyan Shi[1,2]

[1]Department of Bioengineering, University of California San Diego, La Jolla, California
[2]Corresponding author: *L2shi@ucsd.edu*

Published in the Molecular Biology section

Raman microscopy is a vibrational imaging technology that can detect molecular chemical bond vibrational signals. Since this signal is originated from almost every vibrational mode of molecules with different vibrational energy levels, it provides spatiotemporal distribution of various molecules in living organisms without the need for any labeling. The limitations of low signal strength in Raman microscopy have been effectively addressed by incorporating a stimulated emission process, leading to the development of stimulated Raman scattering (SRS) microscopy. Furthermore, the issue of low spatial resolution has been resolved through the application of computational techniques, specifically image deconvolution. In this article, we present a comprehensive guide to super-resolution SRS microscopy using an Adam-based pointillism deconvolution (A-PoD) algorithm, complemented by a user-friendly graphical user interface (GUI). We delve into the crucial parameters and conditions necessary for achieving super-resolved images through SRS imaging. Additionally, we provide a step-by-step walkthrough of the preprocessing steps and the use of GUI-supported A-PoD. This complete package offers a user-friendly platform for super-resolution SRS microscopy, enhancing the versatility and applicability of this advanced microscopy technique to reveal nanoscopic multimolecular nature. © 2024 The Authors. Current Protocols published by Wiley Periodicals LLC.

Basic Protocol: Super-resolution stimulated Raman scattering microscopy with graphical user interface–supported A-PoD
Support Protocol: Deuterium labeling on cells with heavy water for metabolic imaging

Keywords: deconvolution • metabolic imaging • stimulated Raman scattering • super-resolution

How to cite this article:
Jang, H., Li, Y., Wu, S., & Shi, L. (2024). Super-resolution stimulated Raman scattering microscopy with graphical user interface–supported A-PoD. *Current Protocols*, *4,* e970. doi: 10.1002/cpz1.970

INTRODUCTION

Vibrational microscopy, particularly Raman microscopy, holds significant promise in unveiling molecular structural details. Raman microscopy uses visible light sources,

CURRENT PROTOCOLS
A Wiley Brand

Current Protocols e970, Volume 4
Published in Wiley Online Library (wileyonlinelibrary.com).
doi: 10.1002/cpz1.970

making it more versatile for configuring setups with various optical instruments. In theory, Raman scattering signals encompass structural information from every molecule within the sample. Nevertheless, when compared with fluorescence microscopy, this technique yields lower signal levels. To surmount this technical limitation, several approaches have been developed. By generating Raman scattering with one laser beam and stimulating the signal with another laser beam, the signal could be enhanced 10^8 times. This signal-enhancing process is called stimulated Raman scattering (SRS) and has been applied for microscopy (Freudiger et al., 2008). This signal enhancement has made practical imaging of biological samples feasible. However, the relatively modest resolution of SRS remains an obstacle to obtaining subcellular organelle-level information.

Numerous super-resolution microscopy methods have emerged, primarily relying on fluorescence signals (Betzig et al., 2006; Gustafsson, 2000; Hell & Wichmann, 1994; Rust et al., 2006). More recently, a handful of super-resolution techniques for Raman imaging have emerged. However, it is worth noting that the resolution limit of super-resolution SRS is still more than 10 times worse than that of super-resolution fluorescence microscopy. To address this limitation, we have adopted an image deconvolution method (Jang et al., 2023).

Image deconvolution is a computational technique used to recover details in distorted images (Sage et al., 2017; Sibarita, 2005), with blurring being a common type of distortion. Consequently, by solving the inverse problem of the relationship between the blurry images and the function to describe the pattern of blur (point spread function [PSF]), this method has been employed to eliminate blurriness and enhance spatial resolution. Nevertheless, it is important to note that due to potential artifacts that can arise during this process, image deconvolution does not qualify as a super-resolution microscopy technique.

Sparse deconvolution was initially used to address artifacts and reconstruct images in single-molecule localization microscopy (Hugelier et al., 2016; Min et al., 2014; Zhu et al., 2012). However, creating super-resolution images from a single frame of low-resolution images with a high emitter density proved to be a challenging task. To tackle this issue, we developed a more advanced sparse deconvolution algorithm known as Adam-based pointillism deconvolution (A-PoD; Jang et al., 2023). This approach mimics the concept of pointillism painting and describes images with multiple discontinuous spots (virtual emitters). The virtual emitters have the same unit intensity, and the total number of emitters is fixed. This characteristic allows for suppressing artifacts and describes real emitters' distribution. Therefore, from low-resolution images of high-density emitters, super-resolution images can be restored. Accordingly, when applied to SRS microscopy, this method allowed us to achieve a spatial resolution below 60 nm.

BASIC PROTOCOL

SUPER-RESOLUTION STIMULATED RAMAN SCATTERING MICROSCOPY WITH GRAPHICAL USER INTERFACE–SUPPORTED A-POD

The Basic Protocol provides information about how to measure SRS signals from samples and how to convert the images to super-resolution images using A-PoD. To ensure user-friendliness, we have created a graphical user interface (GUI) to support A-PoD. We guide the reader through the critical parameters and conditions necessary to obtain improved super-resolution images using this innovative concept, from the measurement process to the analysis stage.

Materials

Tissue or cell samples (see Support Protocol)
Immersion oil (e.g., Olympus, cat. no. IMMOIL-F30CC)

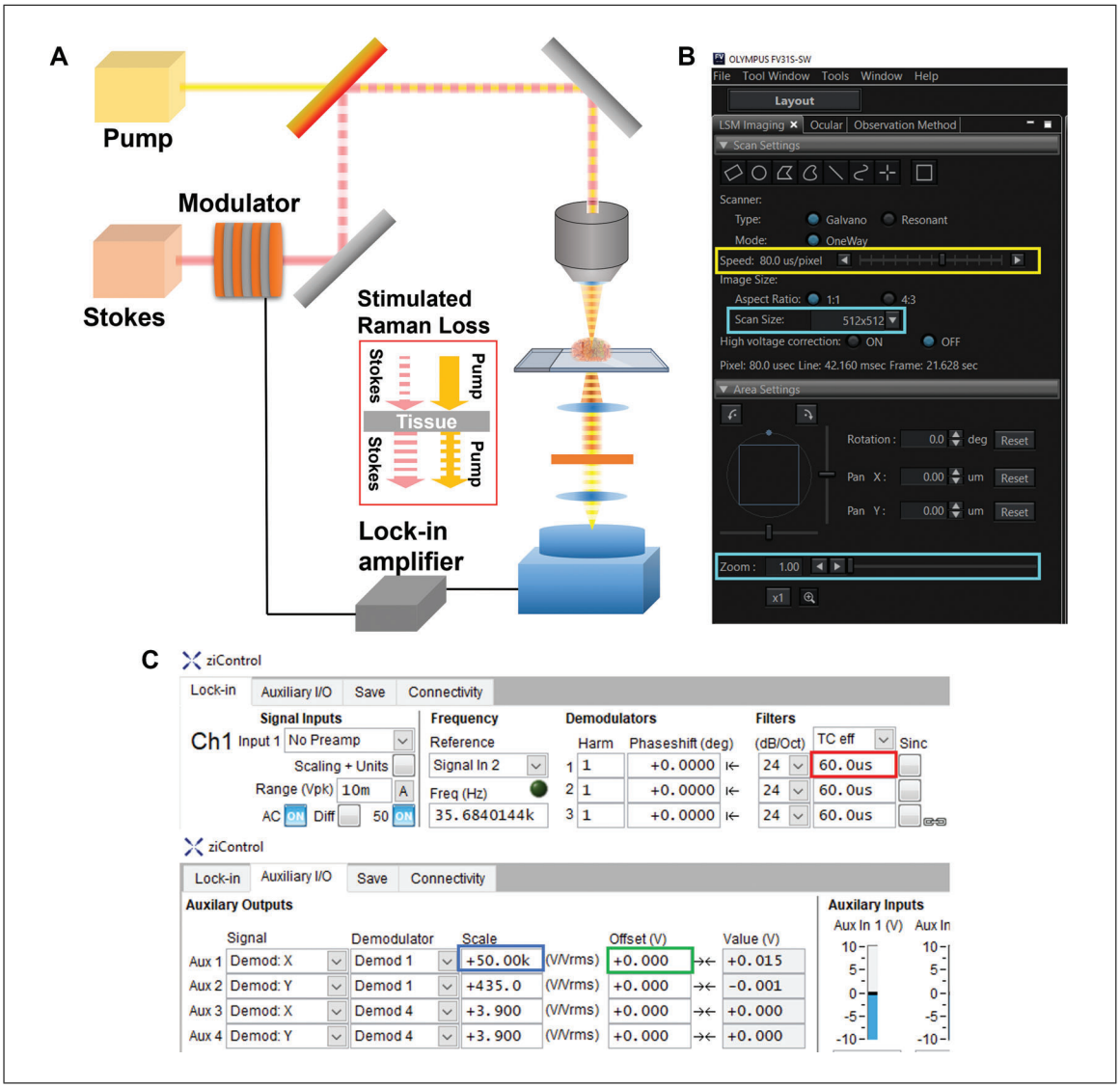

Figure 1 (**A**) Schematic of super-resolution stimulated Raman scattering microscope setup. (**B**) Parameters related to image size, pixel number (cyan box), and imaging speed (yellow box) should be modified. (**C**) Parameters for lock-in amplifier control should be optimized. Red box, time constant; blue box, signal scale; green box, signal offset.

Custom-built upright laser-scanning microscope (e.g., Olympus FV1200MPE) for SRS setup (see Fig. 1A):
  Objective (e.g., Olympus XLPLN, WMP2, 1.05 NA)
  High-numerical aperture (NA) oil condenser (e.g., Olympus 6-U130)
  Photodiode detector (e.g., Hamamatsu S16008-1010)
picoEmerald Laser system (e.g., Applied Physics & Electronics)
Lock-in amplifier (e.g., Zurich Instruments HF2LI)
Computer with minimum requirements (tested with Intel Xeon Gold 5317 CPU, 128 GB RAM, and NVIDIA RTX A4500):
  16 GB RAM
  Intel Core i5 10th Gen
  NVIDIA GTX 1060
ImageJ
Python 3.8.7 (with Tensorflow-gpu 2.6, Numpy 1.20.3, Pillow, Sci-kit image, opencv, pandas)

Measurement

1. Warm up laser and turn on microscope, Si photodiode detector, and photodiode detector.

   Ensure enough time, about 30 min, until the laser can be stabilized enough.

2. Set measurement parameters of microscope and lock-in amplifier.

   Lock-in amplifiers are instruments used to extract signal amplitudes and phases from noisy environments. They use a phase-sensitive detection scheme to measure signals in a defined frequency band and reject all other frequencies or phases. They can accurately measure signals with amplitudes even a million times lower than the noise signals. Set the proper time constant considering the practical scanning speed of setup, about 70% to 80% of the dwell time. Use the following parameters: microscope dwell time, 80 µs (Fig. 1B, yellow box); lock-in amplifier time constant, 60 µs (Fig. 1B, red box). In addition, optimize offset and amplitude of signal (Fig. 1C, red and green boxes).

   In SRS, because the signal is generated by the pump beam and Stokes beam interaction, the signal corresponds to changes in the intensity of the two beams. To detect the signal efficiently, modulation-transfer techniques are employed: One of the beams undergoes amplitude modulation, and the in-phase signal is then detected in the other beam. For this purpose, a lock-in amplifier should be used, and the parameters are precisely controlled.

3. Set laser power (illumination intensity), wavelength, pulse width, and repetition rate (duration of laser pulse).

   The laser power is set at the range of 150 to 600 mW, depending on the signal strength. The wavelength for the pump beam is 780 to 990 nm. The Stokes beam is set at 1031 nm, pulse width at 6 ps, and repetition rate at 80 MHz.

   Detailed parameters of the setup can be varied depending on measurement concepts and hardware specifications.

4. Mount sample on sample stage on an oil drop, and place a large water droplet on top of the sample slide.

   Carefully put oil and water drops so that they will not be mixed.

5. Set size of images considering the wavelength and resolution limit.

   Set the smallest pixel size by increasing the image size and zoom number (Fig. 1, cyan box). The smallest pixel size is the most important factor when A-PoD is applied to enhance spatial resolution.

6. Repeat steps to measure multiple channels with different wavenumbers.

Preprocessing for A-PoD (interpolation, denoising, PSF model generation)

7. Load image files in ImageJ.

8. Denoise images if signal-to-noise ratio is not enough.

   We used PURE-denoise filter (Fig. 2A,B), but other denoising methods can also be applied.

9. Resize images to make pixel size $<$100 nm, and save image as .tif format.

   The recommended maximum interpolation number (digital magnification number at which the image is enlarged) is ∼4 to 5. If the signal level is enough, bilinear or bicubic interpolation can be used to improve spatial resolution of resulting images. In addition, Fourier interpolation can also be used. If the signal-to-noise ratio is high enough, Fourier interpolation can work better. However, if images have strong noise, then Fourier interpolation can generate artifacts of periodic pattern.

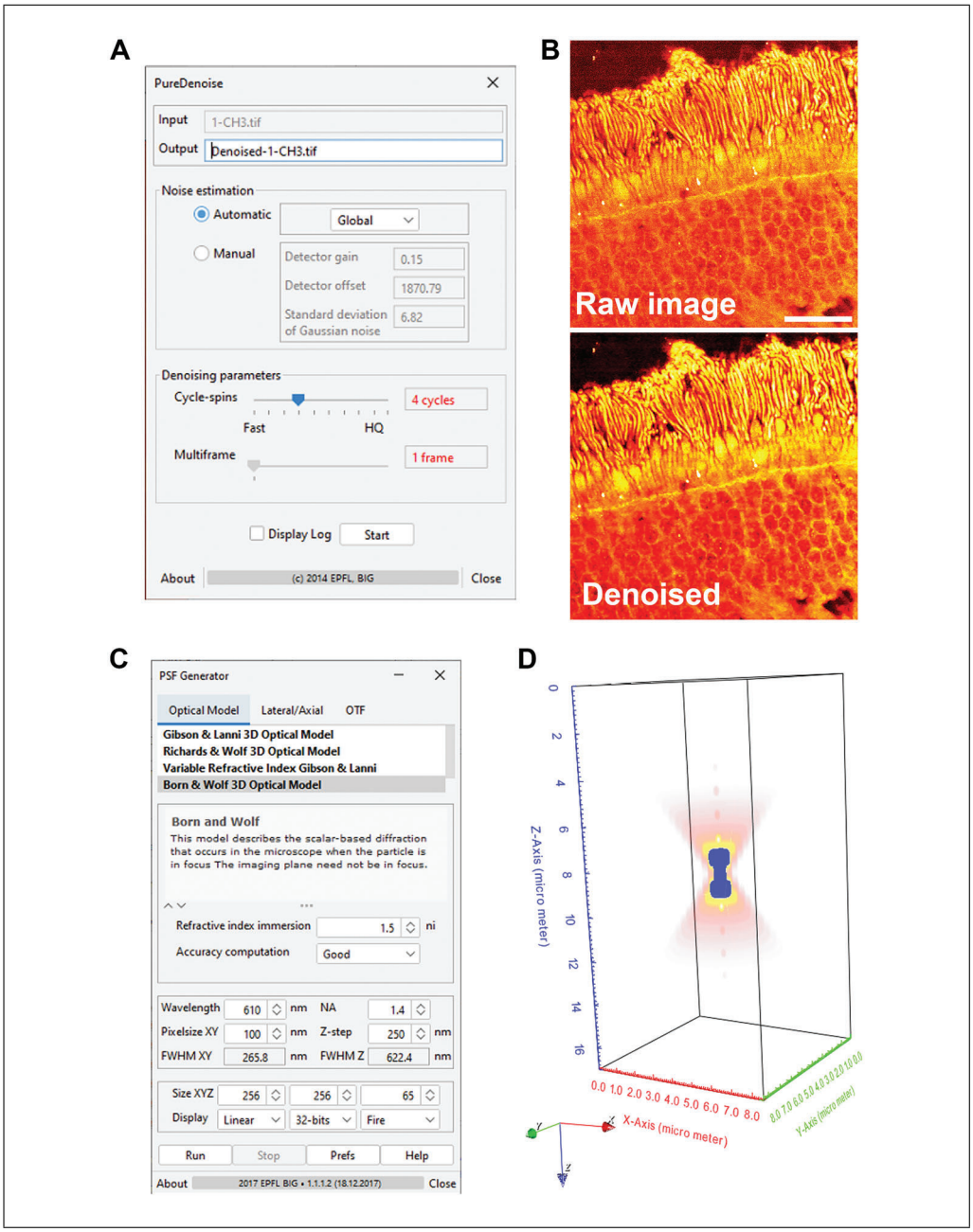

Figure 2 (**A**) Graphical user interface (GUI) of PureDenoise. Parameters can be automatically optimized or can be input manually. (**B**) Raw and denoised images of human retina sample. (**C**) GUI of point spread function (PSF) generator. Using various conditions and PSF model functions, optimized PSF models can be generated. (**D**) Simulation result of pump beam PSF model. Voxel size, 33.3 × 33.3 × 33.3 nm.

10. Install PSF generator plugin.

    The plugin can be downloaded from http://bigwww.epfl.ch/algorithms/psfgenerator/.

11. Run PSF generator, and enter parameters to generate PSF of Stokes beam.

    Since the SRS setup uses two laser beams (Stokes and pump beams), two different PSF models will be generated.

    Set the proper model and parameters, for example, Born and Wolf 3D optical model; refractive index, 1.313; wavelength, 1031 nm; NA, 1.4; pixel size, 33.3 nm, which should be matched with the pixel size of the interpolated images in step 9; z step, 33.3 nm; size XYZ, 512 × 512 × 512. After generating the 3D PSF, for 2D image processing, crop out the focal plane image (Figure 2C).

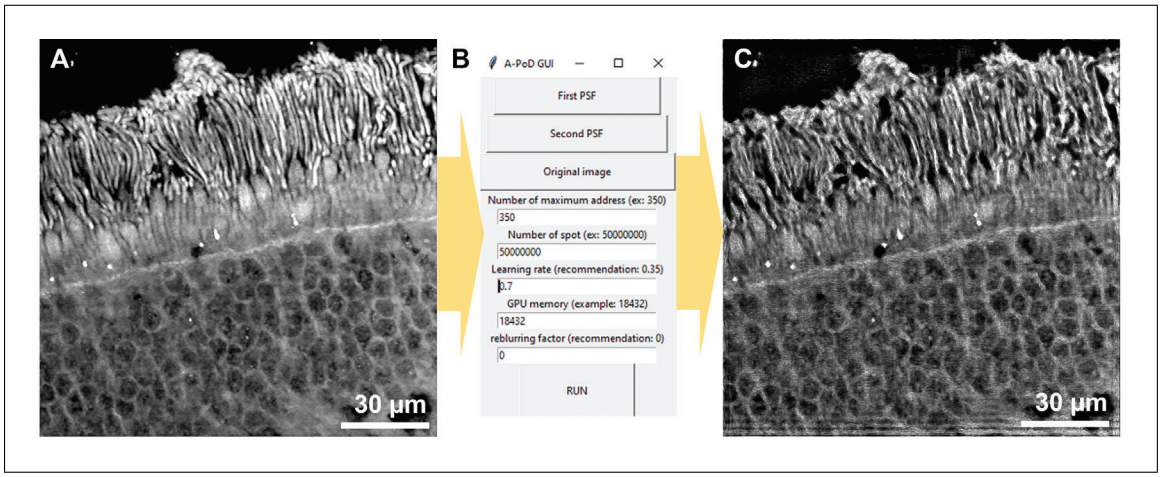

Figure 3 (**A**) Human retina sample image before deconvolution. (**B**) Graphical user interface of Adam-based pointillism deconvolution. The parameters can be input through this window. (**C**) Example deconvolution result of the human retina image.

12. Repeat step 11 to generate PSF of the Pump beam, with a different parameter of wavelength.

    Set the same model and parameters as for PSF generation in step 11, except wavelength. For example, wavelength should be the specific pump beam wavelength (∼780 to 990 nm). After generating the 3D PSF, for 2D image processing, crop out the focal plane image (Fig. 2C).

Installation of A-PoD

13. Install python 3.8.7.

    Some plugins cannot be supported in different versions of python. Therefore, we recommend using the same version.

14. Install plugins (Tensorflow-gpu, Numpy, Pillow, Scikit-image, OpenCV, and pandas).

    Recommended versions of the plugins are Tensorflow-gpu 2.6; Numpy 1.20.3; and the most recent versions of Pillow, Scikit-image, OpenCV, and pandas.

15. Install GPU driver, CUDA, and CUDNN.

    Tensorflow-gpu supports CUDA version 11 only. Accordingly, CUDNN version should be matched with this.

16. Download A-PoD code from Github (*https://github.com/lingyanshi2020/A-PoD*).

    A-PoD_GUI.py: A-PoD for 2D nonlinear microscopy images (SRS and two-photon fluorescence)
    A-PoD_GUI_Single_PSF.py: A-PoD for 2D fluorescence images
    A-PoD_GUI_3D.py: A-PoD for 3D nonlinear microscopy images (SRS and two-photon fluorescence).

Deconvolution using A-PoD (2D SRS images)

17. Run A-PoD_GUI.py.

    After running the file of an image (Fig. 3A), the GUI will pop up as shown in Figure 3B.

18. Set parameters:

    Number of maximum address: proportional constant of virtual emitter number
    Number of spot: maximum number of virtual emitters, which can be localized in a single process

Learning rate: learning rate of Adam solver, which can be controlled from 0.01 to 1

GPU memory: size of GPU memory in Megabyte

Reblurring factor: sigma value of Gaussian function to reblur the resulting image to reduce overfitted results.

19. Click "First PSF," and choose one of the PSF files.

    Choose the PSF file for Stokes beam, which was generated from step 11.

20. Click "Second PSF," and choose another PSF file.

    Choose the PSF file for pump beam, which was generated from step 12.

21. Click "Original Image," and choose image file that will be deconvolved.

    The scale and pixel size of the image should be matched with the scale of the PSF.

22. Press "RUN" button.

    The deconvolution process will be reported through the console window.

23. Open deconvolved file in the folder.

    *The resulting image file (Fig. 3C) will be saved in a "Deconvolved" folder with a file name of "*_A-PoD.tif." If the images contain too much noise, the noise can be minimized by increasing the number of virtual emitters or by increasing the reblurring factor.*

DEUTERIUM LABELING ON CELLS WITH HEAVY WATER FOR METABOLIC IMAGING

SUPPORT PROTOCOL

Metabolic imaging with SRS and deuterium labeling can be applied to various types of animals and cells (Bagheri et al., 2023; Li et al., 2023; Shi et al., 2018; Zhang et al., 2019). The Support Protocol outlines the process for deuterium labeling of cells. Given the diversity in methods for feeding animals and maintaining cells, the specific protocols may vary depending on the cell and animal types. Within this protocol, we focus on elucidating the most common cell culture procedure, which includes the deuterium labeling method.

Materials

Dulbecco's modified Eagle's medium (DMEM) powder

Double-distilled water

Heavy water (deuterium oxide [D_20]; e.g., Cambridge Isotope Laboratories, cat. no. 7732-18-5)

Fetal bovine serum (FBS; e.g., Corning, cat. no. SH300880340)

Penicillin/streptomycin (e.g., Thermo Fisher Scientific, cat. no. 15140122)

HeLa cells (e.g., ATCC, cat. no. CCL-2)

Liquid DMEM (e.g., Corning, cat. no. 10027CV)

70% (v/v) ethanol

1× Dulbecco's phosphate-buffered saline (PBS), no calcium or magnesium (e.g., Thermo Fisher Scientific, cat. no. 14190136)

0.25% trypsin (e.g., Cytiva, cat. no. SH30042.02)

0.4% (w/v) trypan blue, 0.85% (w/v) NaCl (e.g., Lonza, cat. no. 17-942E)

1× PBS, with calcium and magnesium (e.g., Thermo Fisher Scientific, cat. no. 14040117)

16% (w/v) formaldehyde, methanol free (e.g., Thermo Fisher Scientific, cat. no. 28906)

Clear nail polish

15-ml centrifuge tubes (e.g., VWR, cat. no. 89039-664)
Vortex mixer
25-mm syringe filter, 2-μm polyethersulfone (PES) membrane (e.g., Foxx Life Sciences, cat. no. 381-2216-OEM)
Parafilm
10- or 25-cm^2 flask
37°C, 5% CO_2 cell culture incubator
Centrifuge
Hemocytometer (e.g., Millipore Sigma, cat. no. Z359629)
24-well plate (e.g., Fisher Scientific, cat. no. FB0112929)
Poly-D-lysine-coated 12-mm round coverslips
Light microscope
Microscope slides
9-mm diameter imaging spacers
Tweezers, sterile

Medium preparation

1. Weigh and mix 10 mg DMEM powder with 4.7 ml double-distilled water in a 15-ml conical tube. Gently vortex and invert tube to achieve thorough mixing of the solution. To prepare another solution containing heavy water (50% D_2O), instead of 4.7 ml double-distilled water, use 2.35 ml double-distilled water and 2.35 ml heavy water.
2. Add 4.7 ml D_2O, 0.5 ml FBS (5% [v/v] final), and 0.1 ml penicillin/streptomycin (1% [v/v] final). Gently vortex and invert to ensure complete homogenization of the solution.
3. Use a 25-mm syringe filter with 0.22-μm PES membrane to filter media.
4. Seal conical tubes containing media using parafilm, and store at 4°C for up to 3 weeks. Use prewarmed (37°C) media to treat cells in the next section.

Cell labeling

5. To maintain HeLa cells, culture in a 10- or 25-cm^2 flask in standard DMEM supplemented with 10% (v/v) FBS and 1% (v/v) penicillin/streptomycin at 37°C with 5% CO_2.
6. When HeLa cells reach ≥80% confluence, perform subculturing at a 1:10 split ratio.
7. To prepare cells for SRS imaging, when cells reach 80% confluency, rinse once with 1× PBS without magnesium or calcium.
8. Add 2 ml of 0.25% trypsin to detach adherent cells from the flask, and incubate at 37°C with 5% CO_2 for 3 min.
9. Add 2 ml DMEM supplemented with 10% (v/v) FBS and 1% (v/v) penicillin/streptomycin. Gently pipette up and down, and collect cells by centrifuging 3 min at 300 × *g*, room temperature.
10. Resuspend cells in 1 ml DMEM supplemented with 0.5% (v/v) FBS and 1% (v/v) penicillin/streptomycin.
11. Count cells using trypan blue and a hemocytometer under a light microscope, and seed at a density of 2×10^5 cells per well in a 24-well plate with poly-D-lysine-coated glass coverslips.

Alternatively, an automated cell counter can be used for cell counting.

12. Incubate cells at 37°C with 5% CO_2, and gently shake plate to distribute the cells evenly.

13. After 8 hr, gently aspirate original medium using a serological pipet, and add 50% D_2O as prepared in step 1 along the wall of culture well. Return cells to the 37°C, 5% CO_2 incubator for 36 hr.

14. *Optional:* After 36 hr, fix cells on microscope slide:

    Live-cell imaging is possible. If fixed cells are needed, complete these steps.

    a. Prepare microscope slides with 9-mm diameter imaging spacers, and place 15 μl of 1× PBS with calcium and magnesium on spacers.
    b. Rinse cells with 1× PBS with calcium and magnesium.
    c. Add 0.5 ml of 4% (w/v) formaldehyde, methanol free, and leave plate in a biosafety hood for ∼15 min.
    d. Aspirate formaldehyde and rinse twice with 1× PBS with calcium and magnesium.
    e. Add 1.5 ml of 1× PBS with calcium and magnesium to each well.

15. Gently pick up coverslips with sterile tweezers, invert, and place cell-containing side onto the imaging spacers to contact the PBS.

16. Seal outer layer of the coverslip with the imaging spacer using clear nail polish.

COMMENTARY

Background Information

In the past, sparse deconvolution techniques managed data sparsity by incorporating L1 or L0 penalty parameters (Hugelier et al., 2016; Min et al., 2014; Zhu et al., 2012). These methods proved effective for deconvolving images with high emitter densities, particularly in single-molecule localization microscopy. However, the challenge arises in the context of SRS images, which typically exhibit exceptionally high emitter densities. Consequently, conventional sparse deconvolution methods are inadequate for reconstructing super-resolution SRS images. To address this limitation, a Pointillism deconvolution approach (A-PoD) was introduced (Jang et al., 2023). This innovative concept restricts the total number of emitters with the same unit intensity, ensuring a sufficient level of data sparsity required for reconstructing super-resolution SRS images.

One of the primary strengths of SRS imaging lies in its ability to capture multiple molecular signals without labeling. When it comes to measuring various molecular groups and their subtypes, traditional methods often rely on a repeated measurement scheme involving the attachment and detachment of fluorophores. In contrast, SRS microscopy directly captures vibrational signals from numerous functional groups, eliminating the necessity for repetitive labeling processes to detect multiple molecular signals. By acquiring a limited number of channels that represent vibrational modes specific to various functional groups and then separating the spectral overlaps through unmixing, it becomes possible to quantitatively determine the molecular ratios (Lu et al., 2015; Shi et al., 2018).

By combining deuterium labeling with SRS imaging, metabolic activity such as turnover of biomolecules can be measured (Shi et al., 2018; Zhang et al., 2019). When we supply heavy water or deuterated glucose into cells and animals, carbon-deuterium bonds are formed in newly synthesized biomolecules during metabolism, with characteristic Raman peaks in the cell-silent region. In a previous study, we successfully demonstrated the concept of super-resolution metabolic imaging using heavy water. This metabolic imaging approach is now being applied to investigate the effects of aging and diet on metabolism in multiple organs (Li et al., 2023; Li, Bagheri et al., 2022; Li, Chen et al., 2022; Li, Zhang et al., 2022). By combining SRS, deuterium labeling, and A-PoD, we can uncover nanoscopic changes in subcellular organelle-level metabolism induced by factors such as aging, diet, and diseases. Furthermore, to make the approach more broadly applicable, it is essential to create various PSF models tailored to different microscopy setups and imaging systems. After the PSF model

preparations for various imaging setups, achieving A-PoD could serve as a significant milestone in advancing multiple generations of super-resolution imaging techniques.

Furthermore, the A-PoD algorithm holds great potential in a broader context. When the PSF is accurately defined either through theoretical calculations or experimental data, A-PoD becomes a valuable tool for enhancing the spatial resolution of various microscopy images. This improvement extends to diverse imaging modalities, including phase contrast microscopy, photoacoustic microscopy, medical imaging devices, and fluorescence microscopy. Additionally, A-PoD can even enhance the spatial resolution of telescope images. The GUI introduced in this article serves to streamline the A-PoD process, making it more accessible and widening its range of applications.

Critical Parameters

To obtain reliable w and clear images using A-PoD, it is essential to carefully consider several key parameters. First, optimizing the number of virtual emitters is crucial. The A-PoD process mimics pointillism painting concepts. Therefore, resulting images of A-PoD comprise multiple discontinuous spots (virtual emitters). Generally, a greater number of virtual emitters is preferable, but it can also lead to longer processing times. To streamline this parameter's estimation, it is calculated based on the variance and mean value of intensity. Occasionally, manual adjustments may be required, particularly in cases involving strong noise or tilted background signals. For manual corrections, the GUI now includes the option to adjust the "Number of maximum address," typically ranging between 100 and 1000, with increases recommended if noisy results are observed.

Second, because the algorithm employs an Adam solver (Kingma & Ba, 2014), which is a gradient descent algorithm, the learning rate plays a significant role in avoiding local minima and expediting calculations. In this context, the learning rate represents the step size used to move each virtual emitter. If the learning rate is too high, processing times can become longer due to difficulties in precise localization. Conversely, if the learning rate is too low, the results may become trapped in local minima, resulting in artifacts. These artifacts are often related to noise patterns or unique patterns generated by various instrumental conditions.

Lastly, pixel size, referred to as spatial frequency, is critical for accurately localizing virtual emitters. A-PoD lacks the ability to localize within subpixel ranges, and the fitting precision is determined by the pixel size. For instance, if the pixel size is 50 nm, the resolution limit cannot be smaller than 50 nm. Therefore, capturing images with high spatial frequency and a large number of pixels will yield better spatial resolution in the deconvolution results compared with images with lower spatial frequency. Ideally, every sample should be measured with a very high spatial frequency. However, practical constraints like sample integrity and stage stability limit the extent to which we can increase spatial frequency. To address this limitation, interpolation methods, as described in step 9 of the Basic Protocol, can be employed.

Troubleshooting

Most of the problems and challenges are related to the parameters of A-PoD. The representative problems are listed in Table 1.

Time Considerations

The time required for imaging can vary based on factors such as image size and pixel

Table 1 Troubleshooting Guide for A-PoD

Problem	Possible cause	Solution
Strong noise in super-resolution images	Failed optimization due to insufficient number of virtual emitters	Increase parameter "Number of maximum address" or increase reblurring factor
Horizontal or vertical lines on the boundary of images	Signal goes out from the images; partial loss of emitter signal on the boundaries	Add more pixels on the image boundaries, zero-padding
Calculation too slow	Failed optimization due to insufficient number of virtual emitters; too large of a learning rate[a]	Increase parameter "Number of maximum address"; set lower value of learning rate

A-PoD, Adam-based pointillism deconvolution.
[a] Too large of a learning rate can slow down the optimization process.

number. Typically, imaging can take anywhere from a few seconds to several minutes. The time needed for deconvolution with A-PoD also depends on the image quality. For instance, in Figure 3, the deconvolution process for the retina image took <10 min when using a computer with the same specifications mentioned in the materials section.

Acknowledgments

The authors acknowledge the University of California, San Diego startup funds, grants from the National Institutes of Health (U54CA132378, 5R01NS111039, R21NS125395, U54DK134301, U54 HL165443, R01GM149976, NIAID U01AI1 67892, NSF 2320437), and a Hellman Fellow Award.

Author Contributions

Hongje Jang: software, writing—original draft; **Yajuan Li:** resources; **Shuang Wu:** software; **Lingyan Shi:** supervision, writing—review and editing.

Conflict of Interest

A provisional patent application has been filed by the University of California, San Diego patent office for L.S. and H.J. under the title "Super-resolution stimulated Raman scattering microscopy with A-PoD," U.S. provisional application serial no. 63/379,226, filed October 12, 2022. All other authors declare no competing interests.

Data Availability Statement

All the data and source code of this protocol are available with explanation at *https://github.com/lingyanshi2020/A-PoD/*.

Literature Cited

Bagheri, P., Hoang, K., Kuo, C. Y., Trivedi, H., Jang, H., & Shi, L. (2023). Bioorthogonal chemical imaging of cell metabolism regulated by aromatic amino acids. *Journal of Visualized Experiments*, *195*, e65121. https://doi.org/10.3791/65121

Betzig, E., Patterson, G. H., Sougrat, R., Lindwasser, O. W., Olenych, S., Bonifacino, J. S., Davidson, M. W., Lippincott-Schwartz, J., & Hess, H. F. (2006). Imaging intracellular fluorescent proteins at nanometer resolution. *Science*, *313*(5793), 1642–1645. https://doi.org/10.1126/science.1127344

Freudiger, C. W., Min, W., Saar, B. G., Lu, S., Holtom, G. R., He, C., Tsai, J. C., Kang, J. X., & Xie, X. S. (2008). Label-free biomedical imaging with high sensitivity by stimulated Raman scattering microscopy. *Science*, *322*(5909), 1857–1861. https://doi.org/10.1126/science.1165758

Gustafsson, M. G. (2000). Surpassing the lateral resolution limit by a factor of two using structured illumination microscopy. *Journal of Microscopy*, *198*(2), 82–87. https://doi.org/10.1046/j.1365-2818.2000.00710.x

Hell, S. W., & Wichmann, J. (1994). Breaking the diffraction resolution limit by stimulated emission: Stimulated-emission-depletion fluorescence microscopy. *Optics Letters*, *19*(11), 780–782. https://doi.org/10.1364/OL.19.000780

Hugelier, S., de Rooi, J. J., Bernex, R., Duwé, S., Devos, O., Sliwa, M., Dedecker, P., Eilers, P. H., & Ruckebusch, C. (2016). Sparse deconvolution of high-density super-resolution images. *Scientific Reports*, *6*, 21413. https://doi.org/10.1038/srep21413

Jang, H., Li, Y., Fung, A. A., Bagheri, P., Hoang, K., Skowronska-Krawczyk, D., Chen, X., Wu, J. Y., Bintu, B., & Shi, L. (2023). Super-resolution SRS microscopy with A-PoD. *Nature Methods*, *20*(3), 448–458. https://doi.org/10.1038/s41592-023-01779-1

Kingma, D. P., & Ba, J. (2014). Adam: A method for stochastic optimization. *arXiv*, 1412.6980 [preprint]. https://arxiv.org/abs/1412.6980

Li, Q., Chen, Y., Feng, W., Cai, J., Gao, J., Ge, F., Zhou, T., Wang, Z., Ding, F., Marshall, C., Sheng, C., Zhang, Y., Sun, M., Shi, J., & Xiao, M. (2022). Drainage of senescent astrocytes from brain via meningeal lymphatic routes. *Brain, Behavior, and Immunity*, *103*, 85–96. https://doi.org/10.1016/j.bbi.2022.04.005

Li, Y., Bagheri, P., Chang, P., Zeng, A., Hao, J., Fung, A., Wu, J. Y., & Shi, L. (2022). Direct imaging of lipid metabolic changes in Drosophila ovary during aging using DO-SRS microscopy. *Frontiers in Aging*, *2*, 819903. https://doi.org/10.3389/fragi.2021.819903

Li, Y., Bagheri, P., Chang, P., Zeng, A., Hao, J., Fung, A., Wu, J. Y., & Shi, L. (2023). Bioorthogonal stimulated Raman scattering imaging uncovers lipid metabolic dynamics in Drosophila brain during aging. *GEN Biotechnology*, *2*(3), 247–261. https://doi.org/10.1089/genbio.2023.0017

Li, Y., Zhang, W., Fung, A. A., & Shi, L. (2022). DO-SRS imaging of diet regulated metabolic activities in Drosophila during aging processes. *Aging Cell*, *21*(4), e13586. https://doi.org/10.1111/acel.13586

Lu, F. K., Basu, S., Igras, V., Hoang, M. P., Ji, M., Fu, D., Holtom, G. R., Neel, V. A., Freudiger, C. W., Fisher, D. E., & Xie, X. S. (2015). Label-free DNA imaging in vivo with stimulated Raman scattering microscopy. *Proceedings of the National Academy of Sciences of the United States of America*, *112*(37), 11624–11629. https://doi.org/10.1073/pnas.1515121112

Min, J., Vonesch, C., Kirshner, H., Carlini, L., Olivier, N., Holden, S., Manley, S., Ye, J. C., & Unser, M. (2014). FALCON: Fast and unbiased reconstruction of high-density super-resolution microscopy data. *Scientific Reports*, *4*, 4577. https://doi.org/10.1038/srep04577

Rust, M. J., Bates, M., & Zhuang, X. (2006). Sub-diffraction-limit imaging by stochastic optical reconstruction microscopy (STORM). *Nature Methods*, *3*(10), 793–796. https://doi.org/10.1038/nmeth929

Sage, D., Donati, L., Soulez, F., Fortun, D., Schmit, G., Seitz, A., Guiet, R., Vonesch, C., & Unser, M. (2017). DeconvolutionLab2: An open-source software for deconvolution microscopy. *Methods*, *115*, 28–41. https://doi.org/10.1016/j.ymeth.2016.12.015

Shi, L., Zheng, C., Shen, Y., Chen, Z., Silveira, E. S., Zhang, L., Wei, M., Liu, C., de Sena-Tomas, C., Targoff, K., & Min, W. (2018). Optical imaging of metabolic dynamics in animals. *Nature Communications*, *9*, 2995. https://doi.org/10.1038/s41467-018-05401-3

Sibarita, J.-B. (2005). Deconvolution microscopy. *Microscopy Techniques*, 201–243. https://doi.org/10.1007/b102215

Zhang, L., Shi, L., Shen, Y., Miao, Y., Wei, M., Qian, N., Liu, Y., & Min, W. (2019). Spectral tracing of deuterium for imaging glucose metabolism. *Nature Biomedical Engineering*, *3*(5), 402–413. https://doi.org/10.1038/s41551-019-0393-4

Zhu, L., Zhang, W., Elnatan, D., & Huang, B. (2012). Faster STORM using compressed sensing. *Nature Methods*, *9*(7), 721–723. https://doi.org/10.1038/nmeth.1978

Internet Resources

https://github.com/lingyanshi2020/A-PoD

Available A-PoD code repository, including brief instructions on how to install the code.

https://imagej.net/software/fiji/

FIJI (ImageJ) image-processing package; the package can be downloaded and executed without any additional installation.

https://www.python.org/downloads/release/python-387/

Python 3.8.7: A-PoD was mainly written in this language; the package can be downloaded and installed following the instructions.

https://www.tensorflow.org/versions/r2.6/api_docs/python/tf

Tensorflow-gpu 2.6: Python plugin for neural network programming; following the instructions, the package can be installed.

https://pypi.org/project/numpy/1.20.3/

Numpy 1.20.3: Mathematical library for Python; because of the tensorflow-gpu version, use of this specific version is recommended.

https://pypi.org/project/Pillow/

Pillow: Python imaging library; following the instructions, the newest version can be installed on Python.

https://scikit-image.org/

Sci-kit image: Image-processing plugin for Python; this provides a wide range of image-processing capabilities, encompassing both fundamental filtering and sophisticated image clustering functions.

https://pypi.org/project/opencv-python/

OpenCV: Open computer vision library; this library supports multiple functions for advanced image processing.

https://pypi.org/project/pandas/

pandas: Python data analysis library; this library supports functions for data analysis and manipulation.

https://bigwww.epfl.ch/algorithms/denoise/

PURE-denoise filter: Image denoising filter developed by Florian Luisier at the Biomedical Imaging Group (École Polytechnique Fédérale de Lausanne, Switzerland).